

Case study of a road bridge hit by a landslide in highly sensitive clay

Étude de cas d'un pont routier touché par un glissement de terrain en argile extrêmement sensible

L. A. Rødvand

Norwegian Geotechnical Institute, Oslo, Norway

Norwegian University of Science and Technology, Trondheim, Norway

L. Andresen

Norwegian Geotechnical Institute, Oslo, Norway

G. Grimstad

Norwegian University of Science and Technology, Trondheim, Norway

ABSTRACT: After a landslide leading to the partial collapse of the Mofjellbekken (Skjeggestad) motorway bridge in February 2015 an inquiry was established to investigate possible causes of the slope failure. The inquiry concluded that the slide was most likely triggered by a recent filling, placed at the top of the slope. The slope stability calculations, for the inquiry at that time, were carried out using limit equilibrium analyses for calculation of the factor of safety. Site investigations conducted during the bridge construction found highly sensitive clay with a remoulded shear strength under 0.5 kPa in the bottom of the slope. As limit equilibrium methods do not account for the progressive failure mechanism, caused by the strain softening occurring in sensitive materials, new analyses using a finite element model in PLAXIS have been conducted with the NGI-ADPSOFT soil model. The calculated failure load, for the finite element analysis with softening, is compared with the results from the inquiry, and found to be 17 % lower.

RÉSUMÉ: Après un glissement de terrain ayant entraîné l'effondrement partiel du pont autoroutier de Mofjellbekken en février 2015, une enquête a été ouverte pour rechercher les causes possibles de la rupture. L'enquête a conclu que le glissement était probablement dû à un entreposage récent, placé en haut de la pente. Les calculs de stabilité des pentes, nécessaires pour l'enquête, ont été effectués à l'aide d'analyses à l'équilibre limite pour le calcul du facteur de sécurité. Les études de site effectuées pendant la construction du pont avaient révélé la présence d'argile extrêmement sensible avec une résistance au cisaillement remoulée inférieure à 0.5 kPa au bas de la pente. Les méthodes d'équilibre limite ne prenant pas en compte le mécanisme de défaillance progressive, provoqué par le ramollissement des contraintes dans les matériaux sensibles, de nouvelles analyses utilisant un modèle d'éléments finis dans PLAXIS ont été effectuées avec le modèle de sol NGI-ADPSOFT. La charge de rupture calculée, pour l'analyse par éléments finis avec adoucissement, est comparée aux résultats de l'enquête et s'est avérée être inférieure de 17%.

Keywords: sensitive clay; slope stability; FEM; progressive failure

1 INTRODUCTION

On the afternoon of 2nd February 2015 a landslide occurred at Mofjellbekken, Norway with a volume of approximately 10 000 m³ (NVE, 2015). The landslide reached the foundations of a motorway bridge, and caused its partial collapse, after which the authorities immediately closed the bridge. Even at this early stage, it was suspected that sensitive clay was involved in the landslide and the authorities feared that the landslide would propagate further and lead to the full collapse of the bridge.

The Norwegian Water Resources and Energy Directorate (NVE) established an independent investigation committee to find the cause of the landslide. Possible triggering actions including erosion in the stream, rainfall events, traffic vibrations and the placement of a new fill material on the slope were considered. The inquiry concluded that the fill material placed at the slope crest just before the occurrence of the landslide was the cause of the slide (NVE, 2015).

The slope stability analyses conducted by the inquiry used the software GeoSuite Stability (Novapoint, 2015), which is a 2D Limit Equilibrium Method (LEM). Classical LEM is based on perfectly plastic material behaviour (or at least strain compatibility along the slip surface), therefore the method does not account for the progressive failure associated with the post peak softening behaviour observed in the sensitive clay present at this site. This paper investigates the effects of including the strain softening behaviour on the failure of the Mofjellbekken slope.

2 BACKGROUND

2.1 Strain softening

Under undrained loading, sensitive clays display a significant loss of shear strength when loaded beyond their maximum strength. Deformations typically localise into shear bands that experience very large shear strains. The thickness of these shear bands plays a crucial role in the

failure mechanism, as thinner shear bands exhibit more brittle behaviour.

2.2 The progressive failure mechanism

Slides in sensitive clay are progressive in nature and a relatively small triggering event may initiate a large landslide, for example the Rissa landslide in 1978 (Gregersen, 1981). This occurs because soil elements which have passed their peak strength have to redistribute stresses to neighbouring elements as their own strength decreases. Hence the mobilised shear resistance along any potential failure surface at the triggering point of global instability varies, and the average resistance is lower than that predicted by perfectly plastic behaviour.

A study of a fill on a gently inclined sensitive clay slope by Jostad, Fornes, and Thakur (2014) concludes that on average the capacity of that particular slope reduced by 9 % when the strain softening behaviour was included. Similar findings are also seen in Grimstad and Jostad (2012).



Figure 1. Aerial photo of Mofjellbekken landslide

2.3 Anisotropy

Norwegian clays are known to display highly anisotropic behaviour (Bjerrum, 1973 and Karlsrud and Hernandez-Martinez, 2013), and this stress path dependency (anisotropy) of clays has a significant effect on both their strength and

stiffness parameters. The direction of shearing varies along a slip surface, therefore the distinction between active, direct and passive strengths, respectively denoted by s_u^A , s_u^D , and s_u^E , is included in all the models presented in this paper (LEM and FEM).

2.4 Soil conditions

The Mofjellbekken motorway bridges are approximately 230 m long and cross a 25 m deep valley. A small stream flows along the bottom of this valley, see Figure 2. The soil layering (Figure 3) consists of a 3 - 5 m upper layer of weathered dry crust and old fill material from landscaping the area. The soil beneath is classified as a soft to medium stiff silty clay. The depth to bedrock varies greatly in the area, with a deep gorge in the bedrock aligned in the same direction as the valley above. Behind the slope crest the bedrock is around 9 m below the ground surface.

Prior to the bridge construction, highly sensitive clay was discovered in the bottom of the valley, under elevation +94, but was not detected beneath the bridge abutments (NPR, 1997 and NPR, 2000).

The geotechnical site investigations carried out after the landslide, whilst not showing sensitive clay in the slide masses, did show sensitive material higher up in the slope at elevation +99 directly south of the slide (NPR, 2015a). It is supposed that there was a continuous layer of

sensitive clay prior to the slide, which was then disturbed and flowed out of the slope during the slide event, as traces of slide masses (sensitive clay) were found up to 500 m downstream (NVE, 2015).

2.5 Triggering mechanism and slide development

At the time of the slide, new fill material was being deposited on the slope just South-East of the bridges. The investigation approximated this

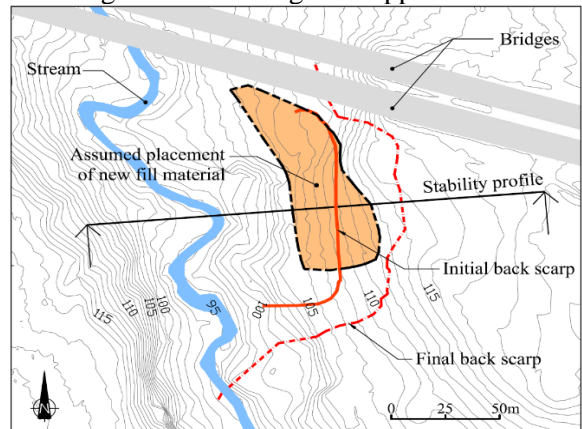


Figure 2. Map of Mofjellbekken landslide fill volume to be approximately 3500 m³, with an average height of 1.5 – 1.6 m. Stability calculations (LEM) by the inquiry (NVE, 2015) demonstrated that the slope had a marginal factor of safety before the landslide, and that the additional load from the new filling reduced it to a level where the occurrence of a slide was inevitable.

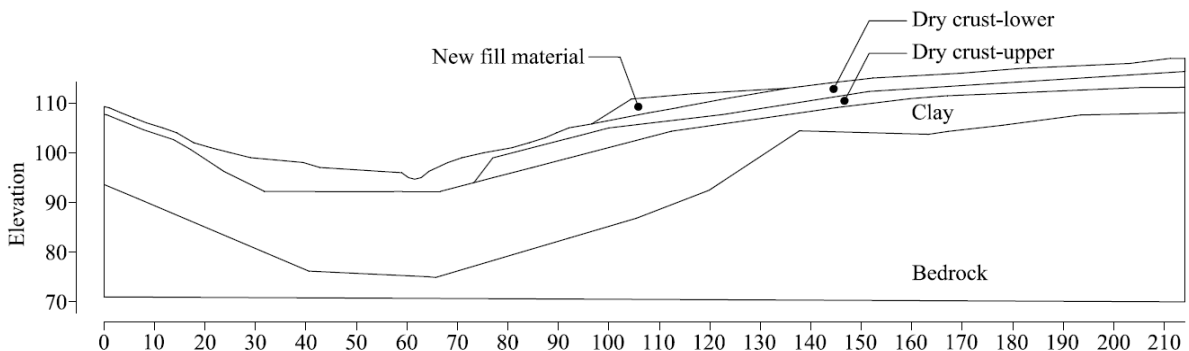


Figure 3. Cross section profile- critical profile for slope stability, position shown in Figure 2.

The slide motion occurred in multiple phases. The initial phase included most of the area covered by the new fill material, see Figure 2. Then the steep back scarp collapsed and propagated the slide backwards, and it was this stage that affected the bridge foundations (dashed red line in Figure 2). This paper looks solely at the initial slide, as the purpose is to investigate the triggering load and the initial slide mechanism.

2.6 Failure mechanism

The shape and depth of the initial slide mechanism have been reconstructed to a reasonable degree of certainty by studying a terrain scan taken just after the slide, and the CPTU conducted in the slide material. These CPTU displayed a drop in tip resistance and side friction at depths consistent with a potential slip surface.

3 NGI-ADPSOFT MODEL

NGI has developed the model NGI-ADPSOFT (Grimstad et al., 2010) which has been implemented as a user defined soil model (USDMM) into the finite element program PLAXIS. It is a total stress based soil model that accounts for shear stress anisotropy and strain softening. A full description of the model without softening, the NGI-ADP model, is found in Grimstad et al. (2012).

3.1 Model parameters

3.1.1 Sensitive clay

The material parameters for the NGI-ADPSOFT soil model were chosen as close as possible to the input used for the limit equilibrium calculation. Shear strength profiles based on results from laboratory tests and interpretation of CPTU were taken directly from the inquiry's report (NVE, 2015), and formed the reference strength input, s_u^0 , presented in Table 1.

Table 1. Input strength profiles for NGI-ADPSOFT model

Profile 1		Profile 2		Profile 3		Profile 4	
x-coordinate = 0		x-coordinate = 43		x-coordinate = 59		x-coordinate = 64	
Elevation	s_u^0	Elevation	s_u^0	Elevation	s_u^0	Elevation	s_u^0
(m)	(kN/m ²)	(m)	(kN/m ²)	(m)	(kN/m ²)	(m)	(kN/m ²)
109	44	97	39	96	39	96	39
103	44	92	39	91	39	91	39
82.5	123	83	66	82	66	82	66
75	123	75	66	75	66	75	66
Profile 5		Profile 6		Profile 7		Profile 8	
x-coordinate = 68		x-coordinate = 100		x-coordinate = 137.7		x-coordinate = 214.1	
Elevation	s_u^0	Elevation	s_u^0	Elevation	s_u^0	Elevation	s_u^0
(m)	(kN/m ²)	(m)	(kN/m ²)	(m)	(kN/m ²)	(m)	(kN/m ²)
98	39	106.5	44	113.5	44	119	44
93	39	100.5	44	107.5	44	113	44
83	66	97.5	54	104.5	54	110	54
75	66	92.5	54	99.5	54	105	54
		87.5	98	94.5	98	100	98
		80	123	87	123	92.5	123

Additional parameters required for the NGI-ADPSOft model were fitted based upon an undrained triaxial compression test (CAUC) on a sensitive clay sample taken from the intact slope just south of the landslide. Figure 4 presents the experimental data (NPRA, 2015b), and the fitted NGI-ADPSOft curve. As no DSS or triaxial extension (CAUE) tests were conducted on Mofjellbekken clay, the choice of direct and passive parameters was based upon results from NGI's block sample database on similar sensitive clays (Karlsrud and Hernandez-Martinez, 2013). The full list of NGI-ADPSOft material parameters is displayed in Table 2.

Parameters for a similar non-softening clay are included in the table. This material will be used later to make a direct comparison with the limit equilibrium calculation result.

3.2 Other soil materials

The dry crust and fill materials were modelled as drained Mohr-Coulomb materials with the properties shown in Table 3, which were chosen based upon the inquiry's material parameters. Bedrock was modelled as a very stiff linear elastic material.

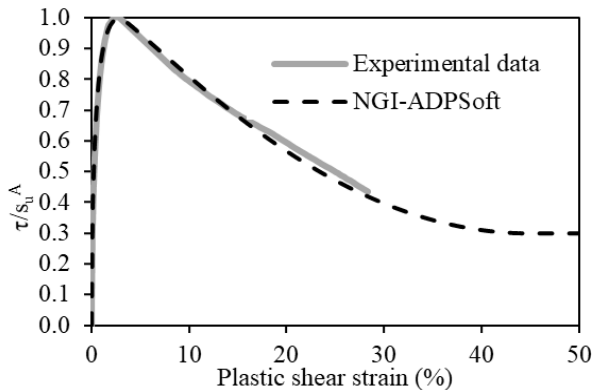


Figure 4. NGI-ADPSOft model curve fitting to CAUC test on sensitive Mofjellbekken clay

4 RESULTS

4.1 The LEM calculation

The stability calculation using LEM is presented in (NVE, 2015 and Haugen, et al., 2016). The calculated safety factor for the slope including the new fill material was 0.99, the failure surface is shown in red in Figure 5.

4.2 The FEM calculation

The calculation is conducted under plane strain conditions with 16948 6-noded elements. Initial conditions in the model were applied using gravity loading. Then the new fill material was activated in a staged construction phase, with the material behaviour set to undrained. The slope failed before the full weight of the new fill material was applied, thereby confirming that the safety factor was under 1.0.

The FEM calculation was performed twice, with identical conditions, apart from the changing the clay layer from non-softening clay to softening clay.

4.2.1 Initial condition

The hardening parameter, κ_1 , is defined by eq. (1), where γ_p is the plastic shear strain and γ_p^p is the plastic "peak" shear strain. The hardening parameter is also directly related to the mobilisation of shear stress, τ , from τ_0 (when $\kappa = 0$) to τ_{peak} (when $\kappa = 1$) and may be used to assess the initial mobilisation (relative to τ_0) of soil in the slope prior to the placement of the fill material. For a strain softening material, this has particular importance as it defines how much additional shear stress the soil material can withstand before it starts to soften.

$$\kappa_1 = \begin{cases} 2 \cdot \frac{\sqrt{\gamma^p / \gamma_p^p}}{1 + \gamma^p / \gamma_p^p} & \text{for } \gamma^p < \gamma_p^p \\ 1 & \text{for } \gamma^p \geq \gamma_p^p \end{cases} \quad (1)$$

Table 2. Input parameters for NGI-ADPSoft materials

Parameter	Description	Non-softening clay	Softening clay
γ_{tot} (kN/m ³)	Total unit weight	19.5	19.5
G_0/s_u^A	Initial and unload/reload stiffness	1000	1000
s_u^A/s_u^0	Active strength normalised by input strength	1	1
ε_p^C (%)	Axial strain at peak in CAUC	2	2
γ_p^{DSS} (%)	Shear strain at peak in DSS	5	5
ε_p^E (%)	Axial strain at peak in CAUE	4.67	4.67
ε_r^C (%)	Axial strain at residual state in CAUC	30	30
γ_r^{DSS} (%)	Shear strain at residual state in DSS	45	45
ε_r^E (%)	Axial strain at residual state in CAUE	30	30
τ_0/s_u^A	Initial mobilisation of max. shear stress	0	0
s_u^{DSS}/s_u^A	Normalised DSS strength	0.73	0.73
s_u^P/s_u^A	Normalised passive strength	0.45	0.45
s_{ur}^A/s_u^A	Normalised residual active strength	1	0.3
s_{ur}^{DSS}/s_u^A	Normalised residual DSS strength	0.73	0.22
s_{ur}^P/s_u^A	Normalised residual passive strength	0.45	0.14
ν'	Drained Poisson's ratio	0.4	0.4
ν_u	Undrained Poisson's ratio	0.495	0.495
c_1	Shape parameter	1.1	1.1
c_2	Shape parameter	1.1	1.1

Table 3. Input parameters for Mohr-Coulomb materials

Parameter	Description	Dry Crust Upper	Dry Crust Lower	Fill material
Material type	Material type used in the calculation	Drained	Drained	Drained
γ_{tot} (kN/m ³)	Total unit weight	19.5	19.5	20
E (kN/m ²)	Young's modulus	30 000	30 000	30 000
ν'	Poisson's ratio	0.4	0.4	0.3
c_{ref} (kN/m ²)	Cohesion	0.1	5	0.1
φ (°)	Friction angle	38	38	35
ψ (°)	Dilatancy angle	0	0	0

Figure 5 shows that the slope, prior to loading is already in a highly mobilised state, and areas with high κ_1 values coincide well with the future mode of failure.

4.2.2 Failure load

Due to the failure of the slope prior to the addition of the full weight of the new fill material, the measure (ΣM_{stage} * fill unit weight) is used

to evaluate the slope capacity, where $\Sigma M_{stage} = 1.0$ equates to the full fill geometry and unit weight of 20 kN/m².

Results for the calculations are presented in Figure 6. For the non-strain softening clay the slope capacity is 18.2 kN/m², whilst for the sensitive clay the capacity reduces to 16.6 kN/m². These equate to reductions of 9 % and 17 % respectively from the original LEM capacity of 20 kN/m².

A reduction in failure load between the LEM and NGI-ADPSoft model with sensitive clay was expected, due to the inclusion of softening, which in effect reduces the average shear resistance along the failure surface, however the reduction in capacity of the non-sensitive clay was not expected, and may be due to limitations imposed on the failure mechanism modelled in LEM as discussed in the next section.

4.2.3 Failure mechanism

The failure mechanisms are identified in Figure 7. There is little difference between the mechanisms for non-softening (blue) and softening clay (green); they overlap for much of the failure surface and only diverge at the back scarp. The LEM failure surface (red) is approximately 2.5 m lower at its deepest point and is shorter in length. This difference can be attributed to the LEM assuming a circular failure surface.

The flatter and longer FEM failure surface agrees better with the mechanism reconstructed from the post slide terrain scan and CPTU. It is well established that finite element modelling generates a more realistic failure surface as it does not have to make *a priori* assumptions about the shape or location of the failure surface. The soil is free to fail in the zones where the soil shear strength is unable to support the additional shear stresses (Griffiths and Lane, 1999). The relatively flat failure surface signifies that the direct shear strength of the clay dominates the soil response, and very little passive resistance to the slide is provided in the clay layer at the toe of the slope.

4.2.4 Mesh dependency

In the FEM calculation conducted for sensitive clay, the mesh size restricts the thickness of the shear band to approximately 60 cm. Whilst the thickness of the shear band in reality is unknown, it is expected to be much thinner, and hence undergo more brittle behaviour. Preliminary calculations using the softening scaling technique (Pietruszczak & Mróz, 1981), result in an even

lower failure load. Lowering the failure load further is unrealistic, given the background information for the slide. This indicates that other factors must play a role in the slope failure. These factors may include stabilising 3D effects, strain rate considerations and local drainage effects. These effects will be explored in future work by the authors.

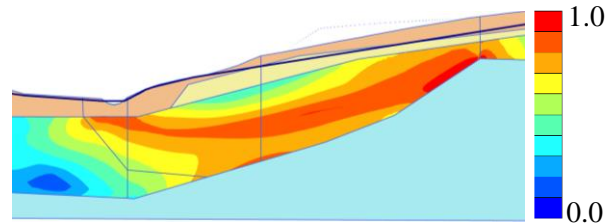


Figure 5. Degree of mobilisation of κ_f in the clay layer prior to the placement of the new fill material

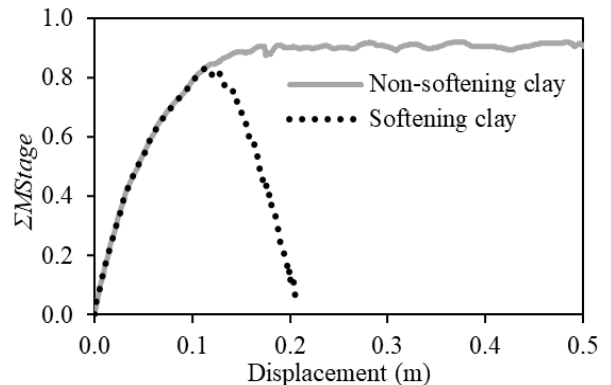


Figure 6. Load-displacement graphs for calculations with and without softening for a point under the new fill material

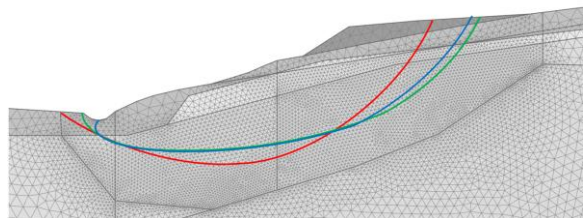


Figure 7. Comparison of failure mechanisms. Red: limit equilibrium. Green: NGI-ADPSoft with softening. Blue: NGI-ADPSoft without softening

5 CONCLUSION

In this paper a comparison of slope stability was made between the limit equilibrium method and the NGI-ADPSOFT model, for a real landslide in sensitive clay. The limit equilibrium calculations were conducted as part of an inquiry into the cause of the landslide. This paper performs finite element calculations using the NGI-ADPSOFT model.

The calculated failure load for the NGI-ADPSOFT model is 17 % lower than that found by the limit equilibrium method. This can be attributed to a combined effect of progressive failure and differences in the predicted failure surface. This disparity demonstrates that a LEM calculation with the peak shear strengths as input will over predict the slope stability because it does not account for the progressive failure mechanism of strain softening clay.

6 ACKNOWLEDGEMENTS

The authors acknowledge the NPRA for allowing the use of the site investigation data. Thank you to my colleagues at NGI: to Khoa D.V. Huynh for invaluable technical support in the use of the NGI-ADPSOFT model, and to Hans Petter Jostad and Marco D'Ignazio for providing many helpful insights. Thanks to NGI and the Norwegian Research Council for providing funding for this research.

7 REFERENCES

- Bjerrum, L. (1973). Problems of Soil Mechanics and Construction on Soft Clays. State-of-the Art Report to Session IV. Moscow: *Proceedings, 8th International Conference on Soil Mechanics and Foundation Engineering*.
- Gregersen, O. (1981). The quick clay landslide in Rissa, Norway. The sliding process and discussion of failure modes. *Proceedings of International Conference on Soil Mechanics and Foundation Engineering*, 421-426. Stockholm.
- Griffiths, D. V., & Lane, P. A. (1999). Slope stability analysis by finite elements. *Geotechnique*, 387-403.
- Grimstad, G., Andresen, L., Jostad, H.P. (2012a) NGI-ADP: Anisotropic shear strength model for clay. *International Journal for Numerical and Analytical Methods in Geomechanics*, 36, 483-497.
- Grimstad, G. & Jostad, H.P. (2012) Stability analyses of quick clay using FEM and an anisotropic strain softening model with internal length scale, *NGM 2012. Proc of the 16th Nordic Geotechnical Meeting. Danish Geotechnical Society*, 675-680.
- Grimstad, G., Jostad, H.P., & Andresen, L. (2010) Undrained capacity analyses of sensitive clays using the non-local strain approach, 9th *HSTAM International Congress on Mechanics, Vardoulakis mini-symposia*, Limassol, Cyprus.
- Haugen, S. B., Henderson, L. A., & Amdal, Å. M. (2016). Case-study of a quick clay landslide that caused the partial collapse of Mofjellbekken bridges in Norway: *Proceedings of the 12th International Symposium on Landslides*. Napoli, Italy.
- Jostad, H. P., Fornes, P., & Thakur, V. (2014). Effect of Strain-Softening in Design of Fills on Gently Inclined Areas with Soft Sensitive Clays. *Landslides in Sensitive Clays: From Geosciences* 305, 305-316. Dordrecht: Springer Science and Business Media.
- Karlsrud, K., & Hernandez-Martinez, F. G. (2013). Strength and deformation properties of Norwegian clays from laboratory tests on high-quality block samples. *Can. Geotech. J.*, 1273-1293.
- Norwegian Geotechnical Institute. (2015). Skredet ved Mofjellbekken bruer. Stabilitetsberegninger. 20150224-01-R.
- Novapoint. (2015). GeoSuite Stability. Version 14.1.1.0.
- NPRA-Norwegian Public Roads Administration. (1997). ZD95C-1-E18 Nordre Vestfold parsell 5B Mofjellbekken bru profil 30152-30370.
- NPRA-Norwegian Public Roads Administration. (2000). ZD950-1A-E18 Nordre Vestfold parsell 5B Mofjellbekken bru øst profil 30141-30359.
- NPRA-Norwegian Public Roads Administration. (2015a). Geoteknikk. E18 Skjeggstadbrua. Datarapport geotekniske grunnundersøkelser. Del 1 - Feltundersøkelser.
- NPRA-Norwegian Public Roads Administration. (2015b). Geoteknikk. E18 Skjeggstadbrua. Datarapport geotekniske grunnundersøkelser. Del 2 - Laboratorieanalyser.
- NVE-Norwegian Water Resources and Energy Directorate. (2015). Skredet ved Mofjellbekken bruer (Skjeggstadskredet). Utredning av teknisk årsaksammenheng. Rapport 53/2015.